Atty. Dkt. No. 016782-0340

## *IN THE UNITED STATES PATENT AND TRADEMARK OFFICE*

Applicant:     Dinand LAMBERTS et al.

Title:     A METAL BURNER MEMBRANE

Appl. No.:     10/553,405

371(c) Date:     10/17/2005

Examiner:     Daniel A. Bernstein

Art Unit:     3743

Confirmation     3705
Number:

### DECLARATION UNDER 37 CFR 1.132

Commissioner for Patents
P.O. Box 1450
Alexandria, VA 22313-1450

Sir:

1. I am a co-inventor of the invention disclosed and claimed in the present patent application (" the present application").

2. I have earned a BSc from Hogeschool Drenthe at Emmen, The Netherlands in June 1988.

3. I have worked at Furigas bv and subsequently at Bekaert Combustion Technology bv since September 2000 and have been engaged in research and development relating to premix gas burner technology.

4. I have reviewed the specifications of U.S. Patent No. 3,122,197 (hereinafter called "Saponara"), U.S. Patent No. 6,149,424 (hereinafter called "Marrecau"), U.S. Patent No. 6,065,963 (hereinafter called "Dewaegheneire"), U.S. Patent No. 2,822,799 (hereinafter

called "Sterick"), and U.S. Patent No. 3,857,670 (hereinafter called "Karlovetz"), and understood them.

5. The invention of the present application is a metal burner membrane configured such that, during use, gas penetrates before being ignited and resulting in visible flames having a lower flame front where the gas initially ignites outside the membrane. The membrane comprises a fabric comprising stainless steel fibers, and comprises a base section having a smallest radius of curvature being $R_{base}$, a closing section, and a transition region connecting the base section to the closing section. The membrane is uninterrupted, wherein the transition region has a smallest radius of curvature $r_{transition}$ being larger than or equal to $0.02 \times R_{base}$ and being smaller than or equal to $0.7 \times R_{base}$.

6. It is my understanding, as a person of at least ordinary skill in this art, that Saponara, Marrecau, Dewaegheneire, Sterick, and Karlovetz, alone or in combination, fail to disclose a metal burner membrane configured such that, during use, gas penetrates before being ignited and resulting in visible flames having a lower flame front where the gas initially ignites outside the membrane, wherein the transition region has a smallest radius of curvature $r_{transition}$ being larger than or equal to $0.02 \times R_{base}$ and being smaller than or equal to $0.7 \times R_{base}$.

**Saponara, Marrecau, Dewaegheneire, Sterick, and Karlovetz fail to disclose a metal burner membrane configured such that gas penetrates before being ignited**

7. Saponara and Marrecau each discloses a radiant burner. A burner operating in a radiant mode is designed to have combustion inside the membrane with substantially no external flame to make the membrane incandescent. Chapter 3 of the Master Thesis *Methane-air combustion on surface burners* provided as Exhibit 1 clearly shows that the temperature of the burner surface is decreasing with an increase in thermal loading (Figure 3.3, page 27). The purpose of a burner working in radiant mode is to generate infrared radiation. This is achieved by having the combustion of the gas inside the membrane, whereby the generated heat immediately heats up the membrane which starts to emit radiation. This effect is reduced with higher thermal loading and is effectively stopped at loads over 1000 kW/m$^2$ (figure 3.3, page 27). The Stephan-Boltzmann law for black body

radiation describes the emission of radiation to be proportional to the fourth power of the absolute temperature of the body. Accordingly, in a radiant burner (such as the ones in Saponara and Marrecau), the intention is to increase the temperature of the membrane by having combustion inside the membrane. Thus, radiant burners are grounded in the physics of black body radiation which relies upon the temperature of the membrane.

8. The present invention is not a radiant burner but relies upon a flame being present outside of the membrane. Such a gas burner operates in the "blue flame mode." The name of the "blue flame mode" finds its roots in natural gas emitting a bluish shine when burning. The blue flame mode is clear from the feature of claim 1 reciting the gas penetrating the membrane before being ignited. In a gas burner operating in a "blue flame mode," the intention is to control the gas flow pattern as the gas is first ejected out of the burner and then the gas is ignited. Chapter 3 of the Master Thesis *Methane-air combustion on surface burners* provided as Exhibit 1 shows that the operation of a surface burner suitable for radiation is only possible if the thermal loading is below 1000 $kW/m^2$. If the air flow is too high, it will blow off the flame. If the fuel gas flow is too low, it will lead to flame extinguishment. The membrane itself serves to distribute the gas but the purpose of a gas burner is to generate heat, and not to increase the temperature of the membrane *per se.* Thus, gas burners are grounded in the physics of fluid dynamics, and do not rely upon the temperature of the membrane. This is also confirmed in Exhibit 2 (Chapter 6 "Lean Premixed Burners" out of "Lean Combustion: Technology and Control, Elesevier Inc., 2008), Section 6.3.2.

9. Futhermore Exhibit 2 Section 6.3.2 mentions that "when the exit velocity exceeds the free-flame burning velocity, the flame must be stabilized aerodynamically to prevent it from becoming unstable" (page 166, lines 12 to 13). The suggestion how this can be done is mentioned lower "Stabilization can be enhanced by perforating the porous surface to allow some the mixture to burn as jet flames, which are stabilized by low velocity hot gases from the surface combustion." (page 166, lines 22-24). The burner surface the co-inventors and myself have invented uses a totally different approach in that the metal burner membrane is so configured that, during use, gas penetrates before being ignited and results in visible flames having a lower flame front where the gas initially ignites outside the membrane, wherein the

transition region has a smallest radius of curvature $r_{transition}$ being larger than or equal to 0.02 x $R_{base}$ and being smaller than or equal to 0.7 x $R_{base}$. In this way a different way of aerodynamic stabilization is achieved. The burner of our invention also solves the drawbacks as mentioned in the last lines of Section 6.3.2 of Exhibit 2 namely the relatively small turndown capacity and large sizes of previous art burners.

10. The difference between the gas burner of present invention working in a blue flame mode and the radiant burner of Saponara and/or Marrecau working in a "radiant mode" is that in the former, the gas penetrates the membrane before being ignited. In other words, the membrane of the present invention does not necessarily heat up appreciably to emit a red glow but relies upon the flame outside the membrane for heating. Conversely, the membrane of Saponara and/or Marrecau relies upon the heating up of the membrane to emit a red glow. This is clear to me from many instances in the text of Saponara ('A radiant burner includes an outer, combustion-sustaining screen which is heated to incandescence' (column 1, lines 46, 47) 'heated to incandescence' (column 1, lines 47) and on many other occasions in the text) and of Marrecau ('heat is radiated to and reflected from the flancs' (the abstract), 'the result is increased radiative output and radiative efficiency' (the abstract), 'the temperature increase of the membrane increases significantly the radiation output of a burner..' (column 2, lines 24 to 29) and again on many other instances in the text).

11. One of ordinary skill in the art would not operate the radiant burners of Saponara and/or Marrecau so as to have gas penetrate the membrane before being initially ignited because the uncombusted gas would lower the temperature of the surface of the membrane, which would run contrary to operating the membrane to reach its optimum temperature for radiant mode operation.

12. If one of ordinary skill in the art further modified the combination of Saponara and Marrecau based on the disclosures of Dewaegheneire, Sterick, and Karlovetz, the basic device would still be a radiant burner, and a radiant burner would not have a metal burner membrane configured such that, during use, gas penetrates before being ignited and resulting in visible flames having a lower flame front where the gas initially ignites outside said membrane.

## Saponara, Marrecau, Dewaegheneire, Sterick, and Karlovetz fail to disclose the transition region of the present invention

13. If one of ordinary skill in the art further modified the combination of Saponara and Marrecau based on the disclosures of Dewaegheneire, Sterick, and Karlovetz, the basic device would still be a radiant burner, which would operate by having gas combust inside the membrane.

14. If the membrane of the resulting combination of Saponara, Marrecau, Dewaegheneire, Sterick, and Karlovetz would be optimized, one of ordinary skill in the art would optimize the resulting combination for its operation as a radiant burner. Saponara discloses that the optimization of the radiant burner would involve optimizing the burner so as to achieve a uniform combustion over the entire inner surface of the radiating membrane. *See* Saponara at column 1, lines 64-72.

15. The present invention relates to a metal burner membrane configured such that, during use, gas penetrates before being ignited and resulting in visible flames having a lower flame front where the gas initially ignites outside said membrane, which is not a radiant burner. The configuration of the present invention permits large variations in gas flow rate through the membrane using the same burner because of the different gas speeds though the burner membrane. *See* the specification at page 3, lines 11-25. Such large variations may decrease the need to have different types of burners on stock. *Id.*

16. Because the radiant burner of the combination of Saponara, Marrecau, Dewaegheneire, Sterick, and Karlovetz has the goal of achieving a uniform combustion over the entire inner surface of the radiating membrane that is in direct conflict with the burner of the present invention which has the goal of achieving large variation in gas flow rate through the membrane, one of ordinary skill in the art would not optimize the geometry of the membrane of the combination of Saponara, Marrecau, Dewaegheneire, Sterick, and Karlovetz to arrive at the geometry of the membrane of the present invention. Accordingly, one of ordinary skill in the art would not optimize the geometry of the membrane of the combination of Saponara, Marrecau, Dewaegheneire, Sterick, and Karlovetz to arrive at the claimed geometrical arrangement of the transition region of the present invention.

17. For these reasons, it is my belief that one of ordinary skill in the art could not have practiced the claimed invention based on the teachings of Saponara, Marrecau, Dewaegheneire, Sterick, and Karlovetz.

18. I hereby declare that all the statements made herein of my own knowledge are true and that all statements made on information and belief are believed to be true; and further, that these statements are made with the knowledge that willful false statements are so made punishable by fine or imprisonment, or both, under Section 101 of Title 18 of the United States Code and that such willful false statements may jeopardize the validity of the application or any patent issuing thereon.
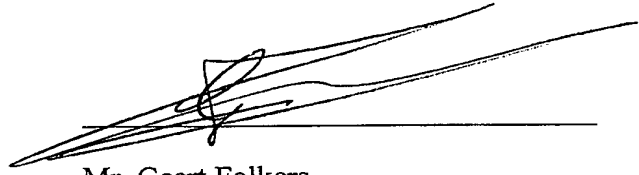
_0 - 7 - 2010_

Date                                                            Mr. Geert Folkers

# **EXHIBIT 1**

A-1

# METHANE-AIR COMBUSTION ON CERAMIC

# FOAM SURFACE BURNERS

PROEFSCHRIFT

ter verkrijging van de graad van doctor aan de
Technische Universiteit Eindhoven, op gezag
van de Rector Magnificus, prof.dr. M. Rem, voor
een commissie aangewezen door het College
van Dekanen in het openbaar te verdedigen op
donderdag 22 mei 1997 om 16.00 uur

door

Peter Hermanus Bouma

geboren te Harlingen

# Chapter 3

# Combustion in the Radiant Mode

## 3.1 Introduction

The radiant mode is discussed in this chapter and in the following chapter. The transport equations and combustion are treated here, while the model used to treat the nitrogen chemistry is presented in the next chapter. The flow through the burner can be assumed to be one-dimensional when the burner is operated in the radiant mode, because a more or less flat flame stabilises on or partly within the burner. Consequently, the governing equations, presented in the previous chapter, are simplified considerably and can be solved by numerical methods.

In Figure 3.1, a schematical view of the burner, operating in the radiant mode, is presented. A premixed methane-air mixture flows through the plenum chamber and the ceramic foam. The plenum chamber is constructed in such a way that the mixture is homogeneously distributed over the burner plate. The mixture velocity $u$ is lower than the adiabatic burning velocity $s_L$ and the flame travels upstream until it reaches the burner. The burning velocity $s'_L$ decreases until it equals the mixture velocity $u$. Finally, a flat flame stabilises on top of the burner or partly within the burner. To decrease the burning
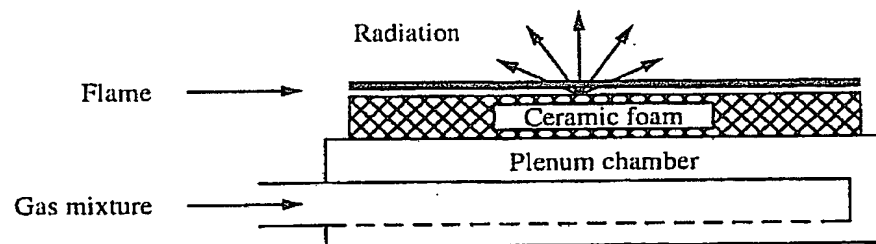


Figure 3.1: *Schematical view of the burner operating in the radiant mode.*

velocity, the flame has to loose energy to the burner. The burner loses this energy by radiation to the surroundings. The burner loses energy to the burner construction by conduction also, but this energy loss is negligible compared to the radiant heat loss.

The outline of this chapter is as follows. In section 3.2 a simple analytical model is presented to study the combustion behaviour in this mode. It is particularly suitable to compute the flue gas temperature and the radiant output. Information about the mass fractions of the chemical components is not available then. In the following section 3.3 a more complete model is presented. The mass conservation equations for the chemical components and the conservation equations of the gas temperature and the solid temperature are given in subsection 3.3.1. The boundary conditions of the computational domain need special attention and are discussed in subsection 3.3.2. The set of equations is discretized on a non-equidistant mesh pattern, described in detail in subsection 3.3.3, where an adaptive second-order exponential conservative discretization technique is used. The results of the analytical and numerical calculations are compared with experimental results. The experimental methods are discussed in section 3.4 and the results in section 3.5. A comparison between the analytical results of the model of section 3.2 and the numerical results is presented in section 3.5 also. In the final section 3.6 concluding remarks are given.

## 3.2   Analytical Model

It appears that the flue gas temperature, the radiant output and/or the surface temperature are of interest for many applications. Especially from a constructing point of view, where a prediction of the thermal load of the construction is of interest, accurate estimates of the temperatures are important. In these cases it would be useful if simple analytical relations would be available to obtain approximations for these variables. Relations for the flue gas temperature $T_b'$ and the surface temperature $T_{surf}$ are derived here. These relations are based on energy conservation, where the energy loss $\Delta E_g$ of the flame is in equilibrium with the energy loss $\Delta E_s$ of the burner [Bou94].

It is assumed that the burner loses energy by radiation to the surroundings. The energy loss by conduction at the burner edges is neglected. The latter assumptions is valid, since the conductivity of the ceramic foam is quite low. However, this is not the case for a metallic burner. For these burners the here presented equations are only valid near the central area of the burner. The net energy loss by radiation per unit area of the ceramic foam burner is given by:

$$\Delta E_s = \epsilon(\sigma T_{surf}^4 - q_{rad,i}) = \epsilon\sigma(T_{surf}^4 - T_{surr}^4), \qquad (3.1)$$

where the radiation is assumed to be concentrated at the outflow interface of the burner. The radiant power of the burner surface is given by the Stefan-Boltzmann law [Sie92], with $\sigma$ the Stefan-Boltzmann constant. The burner surface is assumed to be gray with an effective emissivity $\epsilon$ and has a temperature $T_{surf}$. The incoming radiant flux $q_{rad,i}$ of the surroundings consists of gas radiation (see appendix C) and radiation of the surrounding walls. It is assumed here that the absorbed fraction of the incoming radiation is equal

to the emissivity, which is valid for a gray surface. Gas radiation is neglected for the time being, so that the incoming radiant heat depends on the temperature $T_{surr}$ of the surroundings only.

The energy loss per unit area of the flame depends on the mass flow rate $\rho_g u$ and the difference between the flue gas temperature $T_b'$ and the adiabatic flame temperature $T_b$:

$$\Delta E_g = \rho_g u c_{p,g}(T_b - T_b'), \tag{3.2}$$

with $c_{p,g}$ the (mixture averaged) heat capacity of the flue gases between $T_b'$ and $T_b$. The adiabatic flame temperature depends on the fuel used and the air ratio $n$. The non-adiabatic flame temperature $T_b'$ depends on the unburnt gas mixture velocity $u$, which equalises the non-adiabatic burning velocity $s_L'$ in a stationary situation for a flat flame. The relation between $u$ and $T_b'$ was studied extensively by Kaskan [Kas67] in the sixties. He deduced an empirical relation between the burning velocity and the non-adiabatic flame temperature for premixed flames stabilised on a water-cooled surface burner. For methane combustion he obtained an Arrhenius-like equation between the flame temperature and the burning velocity:

$$u = s_L' = k e^{-E_a/2RT_b'}, \tag{3.3}$$

with $k$ a constant and $E_a$ the overall activation energy. A similar equation can be derived using one-step chemistry [Bus70] and [Lan92] for conduction-controlled flames. Relation (3.3) is obtained by solving the mass and enthalpy balance equations, where the chemical source terms are neglected in the preheating zone ($T_g \leq T_c$). Here is $T_c$ a critical temperature where the chemical source term has the same order of magnitude as the convection and conduction terms. Above the critical temperature ($T_g \geq T_c$), in the reaction layer, the convective terms may be neglected. Relation (3.3) is obtained after matching the solutions at $T_g = T_c$ in the limit of infinite activation energy.

The constant $k$ in relation (3.3) can be eliminated as the (fixed) adiabatic flame temperature $T_b$ and the adiabatic burning velocity $s_L$ are known from experiments [Maa94a] and [Maa94b]. One obtains:

$$T_b' = \left[\frac{1}{T_b} - \frac{2R}{E_a} \ln\left(\frac{u}{s_L}\right)\right]^{-1}. \tag{3.4}$$

It can be shown easily [Goe93] that this relation is valid for all other cooled surface burners, as long as the reaction layer is not in contact with the burner material. However, it remains to be seen whether this is true for the ceramic burner, where part of the reactions may take place inside the ceramic foam. The empirically obtained overall activation energies, the adiabatic flame temperature $T_b$ and the adiabatic burning velocity $s_L$ of atmospheric methane combustion with air are given in Table 3.1 as function of the air ratio $n$. Combining the relations (3.1), (3.2) and (3.4) leads to the following relation between the surface temperature $T_{surf}$ and the gas velocity $u$:

$$T_{surf}^4 = T_{surr}^4 + \left(\frac{\rho_g u c_{p,g} T_b}{\epsilon \sigma}\right) \frac{2RT_b \ln\left(\frac{u}{s_L}\right)}{2RT_b \ln\left(\frac{u}{s_L}\right) - E_a}. \tag{3.5}$$

| $1/n$ | $E_a$ [kJ] | $T_b$ [K] | $s_L$ [cm/s] | $1/n$ | $E_a$ [kJ] | $T_b$ [K] | $s_L$ [cm/s] |
|-------|-----------|-----------|-------------|-------|-----------|-----------|-------------|
| 1.20  | 305       | 2136      | 34.6        | 0.95  | *262*     | 2172      | 34.6        |
| 1.15  | *297*     | 2173      | 37.2        | 0.90  | *253*     | 2120      | 32.1        |
| 1.10  | *288*     | 2210      | 38.3        | 0.85  | *243*     | 2057      | 28.0        |
| 1.05  | *280*     | 2228      | 38.3        | 0.80  | 234       | 1993      | 23.9        |
| 1.00  | 272       | 2220      | 36.7        | 0.75  | *238*     | 1912      | 19.4        |

Table 3.1: *Overall activation energy $E_a$, adiabatic flame tempera-
ture $T_b$ and adiabatic burning velocity $s_L$ of methane-air combustion.
The activation energies in italics are obtained by linear interpolation*
[Kas67]*and* [Maa94a].

Quick estimates of the flame and surface temperature can be made with the relations (3.4) and (3.5) in combination with Table 3.1. The radiant output and the non-adiabatic flame temperature are shown in Figure 3.2 versus the thermal load $P$ (relation (1.2)) per unit area for a methane-air flame with air ratio $n = 1.1$ and for $T_{surr} = 300$ K. The flame temperature increases until the mixture velocity equals the adiabatic burning velocity. Above the adiabatic burning velocity $s_L$ the flame can not stabilise close to the burner and the net radiant output of the burner is zero and the burner surface is cold, as is clearly visible in Figure 3.2. At a low thermal load the radiant output is low, since the mass flow rate is low. Increasing the flow leads to a larger radiant output since the increase of the mass flow rate is larger than the decrease of the temperature difference between $T_b$ and $T_b'$. A further increase of the thermal load leads to a decrease of the radiant output, since the non-adiabatic flame temperature approaches the adiabatic temperature.

The surface temperature is shown in Figure 3.3 for three different emissivities. The uncoated burner has an effective emissivity of approximately 0.4, while the effective emissivity of the coated burner lies between 0.7 and 0.9 [Hoo94]. The surface temperature increases if the emissivity decreases, although the radiant output and the flame temperature remain the same for all three shown $\epsilon$-values. Consequently, the gas temperature inside the foam must increase for a burner with a low emissivity. This indicates that the flame has to stabilise closer to the burner surface, or even partly within the burner. In the most extreme cases the flame can not stabilise and flash-back will occur. The latter phenomena are studied in more detail in chapter 7.

As indicated, this analytical approach can be used only when the reaction layer is essentially outside the burner. For externally cooled burners the flame is stabilised through conductive heat losses only, while for radiant burners other stabilisation mechanisms, based for instance on the volumetric porosity $\phi$, may play a role. When the reaction zone is (partly) within the burner, then the unburnt gas mixture velocity is a factor $(1/\phi)$ larger than outside the burner. Consequently, the burning velocity $s_L'$ has to be a factor $1/\phi$ larger and the flame temperature $T_b''$ (relation (3.4)) should be higher to obtain a stable
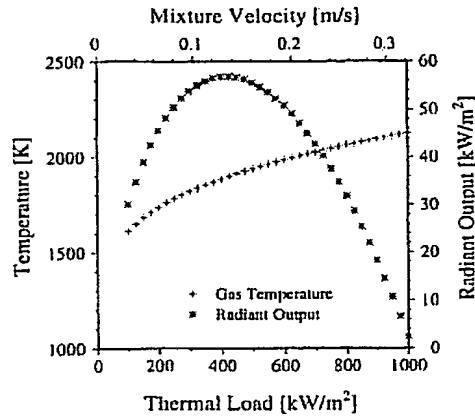
Figure 3.2: *Radiant output and flame temperature of a methane-air flame as function of the thermal load for an air ratio n = 1.1.*
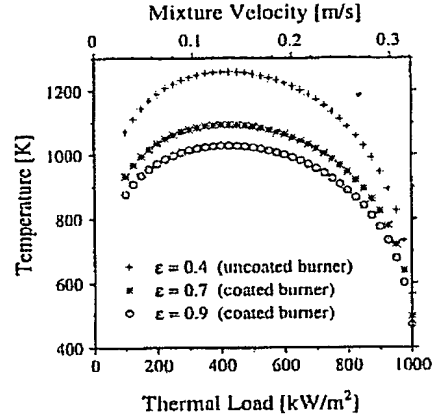
Figure 3.3: *Temperature of the burner surface for three emissivities (ε = 0.4, 0.7 and 0.9) of a methane-air flame as function of the thermal load for an air ratio n = 1.1.*

combustion process. On the other hand, the cooling effect by the burner will be larger when the flame stabilises partly within the burner, since the flame loses energy to the burner in and after the reaction layer. As a consequence, the radiant output is increased and the flame temperature is decreased. Furthermore, the effective conductivity $\lambda_{eff}$, which is responsible for the upstream heat transport of the flame to the unburnt gases, is changed when the flame zone stabilises within the ceramic foam. This will lead to an increase of the burning velocity [Sat89], since the constant $k$ in relation (3.3) is proportional to $\sqrt{\lambda_{eff}}$. The material of the burner used here is believed to be chemically inert. However, for other burner materials, like Zirconia ($ZrO_2$), this is probably not the case. In these cases, heterogeneous reactions may take place at the internal surface, which will change the burning velocity as well. It is clear that several other stabilisation mechanisms than the stabilisation by conductive heat losses may be important when the flame stabilises within the foam. The net effect on the flame temperature and the radiant output cannot be predicted with this relatively simple analytical model and a more sophisticated model has to be used instead. Still, it remains to be seen how these additional effects influence the combustion process on the ceramic foam quantitatively. Experiments have to show the validity of the analytical model (see section 3.4). A more complete model, presented in the next section, may also give more information.

# EXHIBIT 2

Chapter 6

# Lean Premixed Burners

*Robert K. Cheng and Howard Levinsky*

## Nomenclature

| | |
|---|---|
| $A$ | Stoichiometric air factor for a gas |
| $B$ | Thermal load of a burner |
| $F$ | Volumetric flow rate |
| $G_{ang}$ | Axial flux of angular momentum |
| $G_x$ | Axial thrust |
| $H$ | Higher heating value |
| $K$ | Empirical correlation constant |
| $L$ | Swirler recess distance |
| $m$ | Mass flux ratio, $\dot{m}_c/\dot{m}_a$ |
| $\dot{m}_a$ | Mass flux through the annulus |
| $\dot{m}_c$ | Mass flux through the centerbody |
| $q'$ | Two-component turbulent kinetic energy, $[(u'^2 + v'^2)/2]^{1/2}$ |
| $r$ | Radius |
| $R$ | Ratio of centerbody-to-burner radii, $R_c/R_b$ |
| $R_b$ | Burner radius |
| $R_c$ | Center channel radius |
| $Re$ | Reynolds number |
| $S$ | Swirl number |
| $S_L$ | Laminar flame speed |
| $S_T$ | Turbulent flame speed |
| $u'$ | Turbulent rms velocity in axial direction |
| $U$ | Axial velocity |
| $U_a$ | Mean axial velocity through swirl annulus |
| $U_c$ | Mean axial velocity through the center core |
| $U_o$ | Bulk axial flow velocity |
| $v'$ | Turbulent rms velocity in radial direction |
| $V$ | Volumetric flow of air and radial velocity |
| $W$ | Wobbe Index and velocity in radial direction |
| $x_f$ | Leading edge position of the flame brush |
| $x_o$ | Virtual origin of the linearly divergent portions of the axial profiles |
| $Y$ | Blockage of center channel screen |
| $\alpha$ | Blade angle |

$\rho$          Gas density
$\phi$          Equivalence ratio
$\phi_{LBO}$    Equivalence ratio at lean blow-off

## 6.1.  INTRODUCTION

Interest in lean premixed burners as an attractive alternative for "state-of-the-art" practical combustion systems began in the early 1980s. In addition to their common application in $NO_x$ control strategies (Bowman, 1992), these burners were independently introduced in high-efficiency condensing boilers in domestic central heating appliances as a method for the efficient use of the fan, which is necessary to overcome the pressure drop in the condensing heat exchanger. In this sense, these appliances were "low emission" before $NO_x$ emission standards ever existed. In this chapter, we describe a number of developments in the design of lean premixed burners for use in heating applications. As will be discussed, lean premixing presents two challenges to burner design: achieving acceptable flame stability (flashback/blow-off) over the desired range of turndown ratio and maintaining stability with varying fuel composition. Although the effects of fuel variability are well known in gas engines and premixed gas turbines, the analogous principles governing the operation of burner systems are often neglected. Chapter 2 discusses the foundations of some of these principles in general. We shall review them briefly in the particular context germane to lean premixed burners.

## 6.2.  PRINCIPLES OF FUEL VARIABILITY

For the purposes of this chapter, we will only consider the effects of possible variations in fuel composition using natural gas as a fuel because it is by far the most prevalent. For other gaseous fuels, the extension of the basic principles is straightforward. Most of the principles can be traced to older literature (*AGA Bulletin* #10, 1940; von Elbe and Grumer, 1948; Harris and South, 1978) and are general for all burners having some degree of premixing.

Although natural gas is predominately methane with lesser amounts of higher hydrocarbons and inerts, the natural variation in gas composition can have large effects on burner performance. The two largest consequences of this variability pertain to the thermal input and primary aeration of a burner. At a fixed thermal load, fuel gas is supplied in the vast majority of burners at constant pressure drop across a restriction. Since the thermal load of a burner is, by definition, $B = HF$, where $H$ is the calorific or "higher heating" value of the gas (say in $MJ/m^3$) and $F$ is the volumetric flow rate, substituting two gases (1 and 2) at constant pressure changes the thermal load according to:

$$\frac{B_1}{B_2} = \frac{H_1}{H_2}\frac{F_1}{F_2}.$$                         (6.1)

Recognizing that at constant pressure $F$ is inversely proportional to the square root of the density,[1] this suggests that $B \propto H/\sqrt{\rho}$, where $\rho$ is the density of the gas. This relation is used to define the so-called Wobbe Index (Wobbe, 1926) or Wobbe Number,

---

[1] Here, we recall that $F \propto \sqrt{2\Delta P/\rho}$, where $\Delta P$ is the pressure drop over the restriction.

$W = H/\sqrt{\rho}$, where in practice the relative density of the gas (relative to air) is used, giving the Wobbe Index units of energy/volume, similar to the calorific value. Thus, the thermal input to a burner is directly proportional to the Wobbe Index of the gas, not its higher heating value.

When characterizing the system in terms of volumetric flows of fuel and air, we define the primary equivalence ratio, $\phi$, for a given gas as $\phi = AF/V$, where $A$ is the stoichiometric air factor for the gas ($m^3$ air/$m^3$ gas) and $V$ is the volumetric flow of air. Whereas $F \propto 1/\sqrt{\rho}$, for $V$ one can make the distinction between naturally aspirated burners (using a gas nozzle and venturi to entrain combustion air) and fan burners. For naturally aspirated systems, which are also used in some commercial systems to obtain lean equivalence ratios, the amount of air entrained (and thus the volumetric flow rate of primary air, $V$) is solely determined by the momentum flux of the gas jet (von Elbe and Grumer, 1948). The momentum flux of the gas is, to a good approximation, solely determined by the pressure drop over the nozzle. Since the gas pressure is usually not changed when substituting one gas for another, the amount of air entrained, and thus $V$, is independent of the gas composition (Harris and South, 1978). Therefore, since $V$ is constant, for our two gases 1 and 2

$$\frac{\phi_1}{\phi_2} = \frac{A_1 F_1}{A_2 F_2}. \tag{6.2}$$

The calculation of variations in equivalence ratio with Wobbe Index for many natural gases shows that $\phi_1/\phi_2 = W_1/W_2$. This rather surprising result (although known in the older literature, see *AGA Bulletin* #10 (1940) ) can be accounted for by recalling one of the peculiar properties of alkanes, that is, that the air factor divided by the calorific value is constant to within 0.7% for the major alkanes in natural gas. Thus, since $F \propto 1/\sqrt{\rho}$ and $A \propto H$, the right hand side of Equation (6.2) reduces to the ratio of the Wobbe Indices.

The vast majority of practical lean premixed burners use fans to supply the air to the burner. For those systems that do not regulate the air supply by means of an oxygen sensor, the air supply is also independent of the fuel composition, and the relation between Wobbe Index and equivalence ratio is valid. Further, even in industrial combustion equipment that does not employ premixed flames, the *overall* equivalence ratio still varies with Wobbe number, as described above.

Depending on the location, the Wobbe Index can vary by as much as 15% (Marcogaz Ad Hoc Working Group on Gas Quality, 2002). Thus, both the thermal input and the equivalence ratio can also vary by this amount. Obviously, variations of this magnitude can have significant consequences for the efficacy of heating processes, as well as for the stability and pollutant emissions from lean premixed systems (see, e.g., Chapter 2). For stability, the changes in burning velocity caused by the changes in equivalence ratio can create serious challenges to the design of the system in terms of blow-off and flashback.

## 6.3. STABILIZATION METHODS

### 6.3.1. HIGH-SWIRL FLAME STABILIZATION FOR INDUSTRIAL BURNERS

For industrial burners, the primary function of a flame holder is to maintain a stable flame that has high combustion efficiency and intensity throughout the range of turndown for load following. Turndown is the ratio of the peak-to-bottom power outputs

of a given system. Except for some small domestic and commercial appliances where turndown can be achieved by turning the burner on and off intermittently, large industrial and utility systems modulate the power output of the burner (or burners) by adjusting the fuel and the air flows. Therefore, the critical role of the flame holder is to maintain a stable lean flame within a range of flow velocities as well as through the course of rapid changes in flow velocity during transitions from one load point to the next. Typically, industrial systems require minimum turndown of 5:1 (i.e., 100–25% load range), but many advanced processes need turndown approaching 20:1 to enhance system and process efficiencies.

Swirl is the predominant flow mechanism found in premixed and non-premixed combustion systems because it provides an effective means to control flame stability as well as the combustion intensity (Chigier and Beer, 1964; Davies and Beer, 1971; Beer and Chigier, 1972; Syred and Beer, 1974; Lilley, 1977; Gupta *et al.*, 1978). Until now, all practical systems utilized high swirl in which the swirling motion is sufficiently intense (attained beyond a critical swirl number, $S$, and Reynolds number, $Re$) to generate a large and stable central internal recirculation zone that is also known as the toroidal vortex core. Non-premixed burners use the recirculation zone for mixing the fuel and oxidizers to ensure stable and complete combustion. For premixed combustion, the role of the recirculation zone is similar to the wake region of a bluff body flame stabilizer where it retains a steady supply of radicals and hot combustion products to continuously ignite the fresh reactants. Another benefit of using swirling flows for flame stabilization is the generation of a compact flame with much higher combustion intensity than in a non-swirling situation. Syred and Beer (1974) gave an extensive review of the basic processes and practical implementation of two types of swirl combustors. For the sake of clarity, we shall refer to the type of swirling flows that produce strong and well-developed recirculation zones as high-swirl flows, and the burners designed or configured to produce high-swirl flows as high-swirl burners (HSB).

Numerous books, review articles, and a vast number of research papers in both the scientific and engineering literatures attest to the prominent role of high-swirl flows in combustion systems. The overwhelming majority of these studies concentrate on characterizing the size and strength of the recirculation zone as functions of Reynolds and swirl numbers to determine their effects on flame stability and combustion intensity. Flow structures within the recirculation bubble are shown to be highly complex with steep instantaneous velocity gradients producing high intensity non-isotropic shear turbulence. The recirculation bubble also exhibits spatial fluctuations and can swell and shrink from one instance to the next.

The complexity of the recirculation zone structure is a primary cause for the non-linear characteristics of flames generated by HSB. These non-linearities have lesser effects on non-premixed burners and partially premixed burners, but can be detrimental to premixed burners that operate at very fuel-lean conditions for $NO_x$ control. In a typical lean premixed HSB, the flame becomes unstable when $\phi$ is decreased to a limiting value and eventually blows off with further reduction in $\phi$. The instability limit and the lean blow-off limit (expressed in terms of the equivalence ratio at lean blow-off, $\phi_{LBO}$) are non-linear functions of the Reynolds number. Therefore, maintaining low emissions at certain load points can require the burner to operate close to these limits where vortex shedding, mixture homogeneity, and acoustic feedback to the fuel or air systems can trigger larger flame instabilities and premature blow-off. The onset of flame instabilities when coupled with the acoustics mode of the combustion chamber often produces large
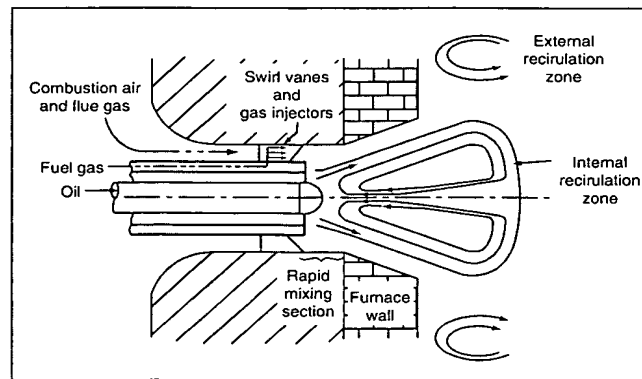
**Figure 6.1** Schematic of RMB.

amplitude oscillations. If unmitigated or uncontrolled, combustion oscillations can lead to rapid hardware degradation and even catastrophic system failure. This sensitivity of lean premixed HSB designs near their lean limit has given rise to the expectation that lean combustion is inherently unstable. As a result, elucidating the basic processes responsible for initiating and sustaining combustion instabilities as well as the development of passive and active control methodologies for combustion oscillations are significant current topics of combustion research. Chapter 7 discusses such oscillations in the context of recirculation-stabilized flames. We will see, however, that appropriately designed fluid mechanics within the burner can substantially reduce sensitivity to lean operation.

Despite the challenges in stabilizing lean premixed turbulent flames, combustion equipment manufacturers have succeeded in developing "fully premixed" HSB that attain <9 ppm $NO_x$ (at 3% $O_2$) emissions. One example is the Rapid-Mix Burner (RMB) manufactured by Todd Combustion, a schematic of which is shown in Figure 6.1. As its name implies, the key feature of the RMB is to inject a homogeneous mixture of reactants in the shortest distance possible. This is to address the major concern of flashback in fully premixed burners. The RMB approach is to integrate the fuel injection port into the swirl vanes. To mitigate $NO_x$ below 9 ppm $NO_x$, this burner relies on introducing flue gas to dilute and slightly preheat the air stream. Other designs such as the Coen Micro-$NO_x$ burners and Net-Com's Hyper-Mix burners utilize multistaged combustion. The basic premise is to create a fuel-rich central combustion zone to serve as a stable pilot to ignite the fuel-lean premixture injected into the surroundings. Several sets of air and fuel injectors are needed to produce and control the fuel-rich/fuel-lean sequence. Additionally, a recirculation zone in the central region is necessary to entrain flue gases into the fuel-rich combustion core to reduce the peak temperatures and in turn provide a means for $NO_x$ control.

## 6.3.2. SURFACE-STABILIZED LEAN PREMIXED INDUSTRIAL BURNER CONCEPTS

Surface-stabilized, or surface-radiant, burners use perforated ceramic tiles, ceramic foam, or porous metal fiber materials to support lean premixed combustion. The operating principle of the surface-stabilized burner is essentially identical to that of the water-cooled sintered burner used in fundamental combustion research (Mokhov

and Levinsky, 2000). By reducing the exit velocity of the premixed fuel–air mixture below that of the free-flame burning velocity, the flame transfers heat to the burner (Botha and Spaulding, 1954), lowering the flame temperature and thus the $NO_x$ emissions. The scale of the porous medium is generally the same as, or smaller than, the laminar flame thickness (of <1 mm), preventing the flame from flashing back inside the material. This method is distinct from submerged radiant combustion (Rumminger et al., 1996), in which the flame is located within the open porous structure. In the submerged case, there is also substantial heat transfer to the burner surface downstream of the primary flame front. For surface radiant burners, the heat transferred to the burner surface is subsequently radiated to the surroundings. Increasing the exit velocity of the combustible mixture reduces the heat transfer to the burner surface (and increases the $NO_x$ emission). When the exit velocity exceeds the free-flame burning velocity, the flame must be stabilized aerodynamically to prevent it from becoming unstable. Because of this relation to the laminar burning velocity (Mokhov and Levinsky, 2000), in the "radiant mode" (exit velocity lower than the free-flame burning velocity), the specific power is limited to $<1\,MW/m^2$. At low exit velocities, the flame temperature becomes so low that the flames extinguish (Mokhov and Levinsky, 1996). This limits the lowest achievable specific power input to $\sim100 - 200\,MW/m^2$. Interestingly, in this mode the flame properties (temperature, $NO_x$ emissions) are independent of the nature of the surface (Bouma and de Goey, 1999; Mokhov and Levinsky, 2000).

Depending on the design for stabilization, a few megawatts per meter square is an average maximum before the flames become unstable. Stabilization can be enhanced by perforating the porous surface to allow some of the mixture to burn as jet flames, which are stabilized by low velocity hot gases from the surface combustion. Scaling is usually accomplished by increasing the surface area (i.e., constant velocity scaling) and consequently the physical size of surface-stabilized burners is directly proportional to the power output. Clearly, for commercial and industrial systems of even a few megawatts, this requires an inconveniently large burner surface. This characteristic is quite unlike that of typical burner designs where constant velocity and constant area scaling (i.e., increasing throughput of reactants to attain high power output) are both applicable. The high cost of some of the porous materials and their fragile nature had limited their use in the past to high-end residential, commercial, and industrial applications. With the development of tough and inexpensive ceramic foams and moderately priced metal fabrics that are pliable and less fragile, more affordable surface-stabilized burners are being marketed to meet a wide variety of utilization needs. Currently, ceramic foam burners are a standard feature in European domestic condensing boilers, where a turndown ratio of 6:1 is reliably achieved over the range of distributed gas compositions.

In addition to emitting very low $NO_x$ concentrations and enhancing radiative heat transfer, the main advantage of surface-stabilized burners is that their shapes can be customized to meet the specific (radiant) efficiency and system requirements of various industrial processes. As mentioned above, the main drawbacks, however, are their relatively small turndown capacity and large sizes.

## 6.3.3.  Low-Swirl Stabilization Concept

The low-swirl burner is a recent development originally conceived for laboratory studies on flame/turbulent interactions (Chan et al., 1992; Bedat and Cheng, 1995;

Cheng, 1995; Plessing *et al.*, 2000; Cheng *et al.*, 2002; Shepherd *et al.*, 2002; Kortschik *et al.*, 2004; de Goey *et al.*, 2005). Its operating principle exploits the propagating nature of turbulent premixed flames, and its basic premise is to stabilize a turbulent premixed flame as a stationary "standing wave" unattached to any physical surfaces. This is accomplished by generating a divergent flow that is formed when the swirl intensity is below the vortex breakdown point. Therefore, the low-swirl burner concept is fundamentally different from the high-swirl concept where vortex breakdown is a vital prerequisite to producing a strong and robust toroidal recirculation zone.

The original low-swirl burner for laboratory studies known as the jet-LSB is shown in Figure 6.2 (Bedat and Cheng, 1995). This burner consists of a cylindrical tube of 5.08 cm ID fitted with a tangential air swirler section located 7 cm upstream of the exit. The swirler consists of four small jets of 0.63 cm ID inclined at 70° to the central axis. Reactants supplied to the bottom of the tube through a turbulence generating plate interact with the tangential air jets. The size of the air jets is kept small so that the swirling fluid motion clings to the inner wall and does not penetrate deep into the reactant core. When the flow exits the burner, centrifugal force due to the swirling motion causes the central non-swirling flow to expand and diverge. The divergent center region is characterized by a linear velocity decay and this feature provides a very stable flow mechanism for a premixed turbulent flame to freely propagate and settle at a position where the local velocity is equal and opposite to the turbulent flame speed (see Chapter 2 for discussion of some of the elements governing turbulent flame speed). Varying the stoichiometry of the reactants (without changing the mean velocity and swirl rate) simply shifts the flame brush to a different position within the divergent flow. This behavior is similar to the behavior of flames stabilized in the divergent regions produced in stagnating flows, but the absence of a downstream stagnation plate or plane in the low-swirl burner allows it to support flames that are much leaner than is possible in stagnation burners.

For practical applications, the LSB approach has many desirable attributes. Its capability to support very lean premixed flames is of course the primary motivation. The features of the flame stabilization mechanism also address the important operational and safety concerns regarding the use of fully premixed burners for industrial processes. The flame cannot flashback into the burner when the velocity at the exit is
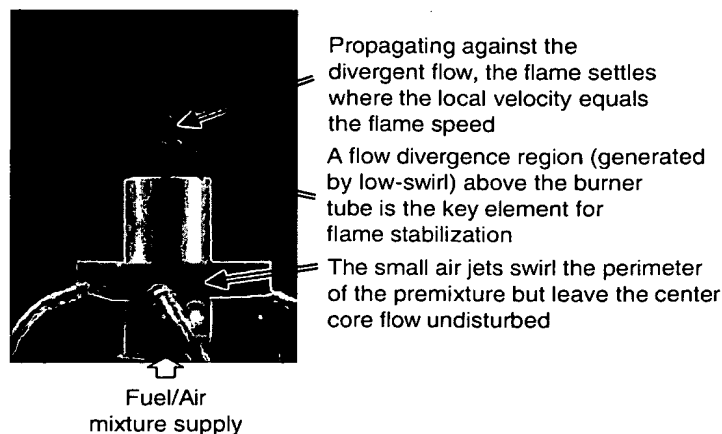


Propagating against the divergent flow, the flame settles where the local velocity equals the flame speed

A flow divergence region (generated by low-swirl) above the burner tube is the key element for flame stabilization

The small air jets swirl the perimeter of the premixture but leave the center core flow undisturbed

Fuel/Air
mixture supply

**Figure 6.2** A jet-LSB demonstrates the principle of low-swirl flame stabilization.

higher than the turbulent flame speed. Blow-off is also mitigated because the flame retreats to a lower velocity region in the divergent flow when any sudden decrease in stoichiometry occurs. Additionally, the consequence of changes in mixture inhomogeneity or slight flow transients is a slight shift in the flame position. Therefore, the likelihood of catastrophic flameout is reduced substantially. The LSB flowfield provides automatically a robust self-adjusting mechanism for the flame to withstand transients and changes in mixture and flow conditions.

One of the first issues for practical adaptation of the LSB is to determine the effect of an enclosure on the flame stabilization mechanism and flame behavior. Figure 6.3 displays centerline velocity profiles from LDV measurements of $CH_4$/air flames at $\phi = 0.8$ and a bulk flow velocity of $U_o = 3.0$ m/s (18.5 kW) generated by the jet-LSB of Figure 6.2 inside quartz cylinders of 7.62 cm diameter and 20 and 30 cm lengths, with or without an exit constriction of 5.4 cm (Yegian and Cheng, 1998). The features of the mean axial velocity profiles (top) in the nearfield region ($x < 50$ mm) are similar to those measured in stagnation burners (Cho *et al.*, 1988; Kostiuk *et al.*, 1993) where flow divergence away from the burner exit is illustrated by a linear decay of $U$ with increasing $x$ followed by an abrupt upturn due to combustion-generated flow acceleration within the flame brush. The inflection point marks the leading edge of the flame brush and provides a convenient means to determine the turbulent flame speed $S_T$. Differences in the enclosed and open LSB profiles are shown in the farfield region where the open flame sustains a higher mean velocity while velocities in the enclosures are lower. This is due to the open flame generating a jet-like plume and the plumes of the enclosed flames expanding to fill the enclosure volume. These data show that the LSB flames are not sensitive down to at least this 3:1 diameter ratio enclosure.

Technology transfer and commercial implementation of low-swirl combustion began with adaptation to residential pool heaters of 15–90 kW (50–300 K Btu/h). These small domestic appliances are commodities and can only afford to include very simple and low cost technologies controlled by rudimentary electronics. The jet-LSB requiring two flow controls was too elaborate, which motivated the development of a simpler burner
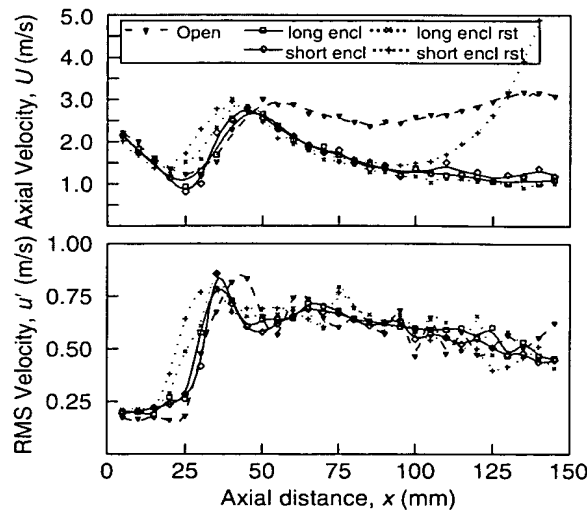


Figure 6.3   Velocity profile from (from Yegian and Cheng, 1998) showing that enclosures have little effect on the flame stabilization mechanism of a jet-LSB for a $CH_4$/air flame with $\phi = 0.8$ at 18.5 kW.

that is easy to manufacture and requires few controls. The outcome was a patented vane swirler (Cheng and Yegian, 1999) that has since been adapted for industrial burners and gas turbines.

The main challenge in developing a swirler for LSB was lack of knowledge on the fluid mechanics of low-swirl flows because all prior research focused on high swirl. Laboratory experimentation with LDV led to the design of Figure 6.4. This LSB is sized for domestic heaters of 18 kW and has a radius $R_b$ of 2.54 cm. It has an annular swirler that consists of eight blades inclined at 37.5° with respect to the burner axis. Its unique feature is an open center channel ($R_c = 2$ cm) to allow a portion of the reactants to bypass the swirl annulus. The center channel is fitted with a perforated screen (3 mm holes arranged in a rectangular grid to give 81% blockage) to balance the flow split between the swirled and the unswirled flow passages. The screen also produces turbulence in the center unswirled core. The swirler assembly is recessed from the exit at a distance $L$ of 6.3 cm. This vane LSB produces the same key flowfield features as the jet-LSB and as shown in Figure 6.5, the flame generated by the vane LSB is lifted with a bowl shape slightly different from the one produced by the jet-LSB. The vane LSB was
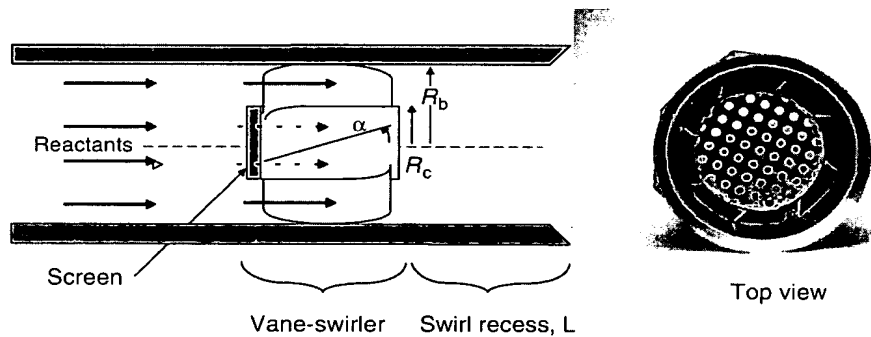


**Figure 6.4** Schematic and photograph of a vane swirler developed for the low-swirl burner.



**Figure 6.5** A vane LSB firing at 18 kW.

found, however, to have very high turndown (approaching 60:1) and very low emissions. More importantly, the design is scalable (Cheng *et al.*, 2000) and the development of scaling rules is crucial to its smooth transition to commercialization in larger industrial systems.

### 6.3.3.1.  Scaling of LSB to Industrial Capacities

Central to the scaling rule for low-swirl vane burners is a new definition of swirl number, $S$, that includes the flow through the center channel. It is derived from the formal definition of $S$ based on the geometry of the device (Syred and Beer, 1974):

$$S = \frac{\text{axial flux of angular momentum}}{\text{axial thrust} \times R} = \frac{G_{\text{ang}}}{G_x R}.$$                (6.3)

Assuming that the distribution of the axial flow remains flat, and that $U$ and $W$ at the burner exit are kinematically related to the blade angle as $\tan \alpha = U/W$, the axial flux of angular momentum in the annular section can then be written as follows:

$$G_{\text{ang}} = 2\pi\rho \int_{R_c}^{R_b} U_a(U_a \tan \alpha) r^2 dr = 2\pi\rho U_a^2 \tan \alpha \left( \frac{R_b^3 - R_c^3}{3} \right).$$                (6.4)

Here, $U_a$ is a mean axial velocity supplied through the swirl annulus. By assuming a flat axial velocity distribution, the linear momentum flux from the two regions of the burner is then calculated as follows:

$$G_x = 2\pi\rho \int_{R_c}^{R_b} U_a^2 r dr + 2\pi\rho \int_0^{R_c} U_c^2 r dr = \pi[\rho U_a^2(R_b^2 - R_c^2) + \rho U_c^2 R_c^2],$$                (6.5)

where $U_c$ is the mean axial velocity through the center core. With Equation (6.3) as defined, the geometric swirl number for the vane swirl burner is then

$$S = \frac{\frac{2}{3}\tan \alpha(1 - R^3)}{\left( 1 - R^2 + \dfrac{U_c^2}{U_a^2}R^2 \right)} = \frac{2}{3}\tan \alpha \frac{1 - R^3}{1 - R^2 + [m^2(1/R^2 - 1)^2]R^2}.$$                (6.6)

Here, $R$ is the ratio of the centerbody-to-burner radii $R = R_c/R_b$. Equation (6.6) is simplified further when $U_c/U_a$ is expressed in terms of $m$, the mass flux ratio (flow split) $m = \dot{m}_c/\dot{m}_a$ through the centerbody ($\dot{m}_c$) and annulus ($\dot{m}_a$); $m$ is the same as the ratio of the effective areas of the center core and the swirl annulus, and can be determined simply by the use of standard flow pressure drop procedures. Obviously, Equation (6.6) is a more convenient form of the swirl equation for engineering design than is provided by Equation (6.3).

The scaling rules were determined from studying the influences of $S$, $L$, and $R_b$ on burner performance using lean blow-off, flame stability, and emissions as the criteria. To start, the LSB prototype shown in Figure 6.4 was used as a benchmark with its swirl number varied by using four different screens with 65–75% blockage. The swirl numbers were $0.4 < S < 0.44$ corresponding to $m$ of 0.8–1, meaning that 44–50% of the reactants bypassed the swirl annulus. These swirlers were fitted with recess distance $L$ from 4 to 12 cm. The 16 LSBs with various $S$ and $L$ combinations were tested with

$CH_4$/air flames at $5 < U_o < 25\,\text{m/s}$ covering a thermal input range of 18–90 kW. All burners were found to be operable. Increasing $S$ pulled the flame closer to the burner, but the lean blow-off remained relatively unaffected, indicating that the performance of the LSB is not highly sensitive to small variations in $S$. The differences were mainly in flame positions and fuel/air equivalence ratio at lean blow-off, $\phi_{LBO}$. Large swirler recesses resulted in a highly lifted flame, but the overall flame stability remained relatively unchanged. A short recess distance produced higher $\phi_{LBO}$, indicating a compromise in the capability to support ultra-lean flames.

Additional studies were performed to explore the effects of varying radius $R_b$ as well as $R$ (0.5–0.8) and $\alpha$ (30–45°). The swirl numbers of the burners with various combinations of $R_b$, $R$, and $\alpha$ were varied by fitting them with screens of different blockages. The most significant finding was that the LSBs with larger $R_b$ operated at the same range of $S$ (around 0.4–0.5) as the smaller burner. Their performances in terms of flame stability and $\phi_{LBO}$ were also identical. Moreover, decreasing $R$ had no effect on emissions or performance but brought about a significant benefit in lowering the pressure drop of the LSB. This can be explained by the fact that reducing $R$ enlarges the swirl annulus and lowers its drag. To maintain a swirl number of 0.4–0.5, a screen with lower blockage is required. For example, the screen used for $R_b = 6.35\,\text{cm}$ with $R = 0.5$ has a 60% blockage compared to 65–81% needed for $R = 0.8$. This combination effectively lowers the overall pressure drop of the burner. The drag coefficients determined for the different LSBs show them to depend only on $R$ and to be independent of $R_b$. This knowledge is very important for engineering LSBs to meet various system requirements and efficiency targets.

The scaling rules for the LSB were established from the above results. They are independent of burner radius (up to $R_b = 25.4\,\text{cm}$). For stable and reliable operation, the $S$ of an LSB should be between 0.4 and 0.55. The swirler can have straight or curved vanes with angle $\alpha$ from 37° to 45°. The center channel-to-burner radius ratios $R$ can range between 0.5 and 0.8. Once $\alpha$ and $R$ are defined, the blockage of the center channel screen can be varied to give $Y$ within the desired range of 0.4–0.5. In addition, the swirl recess distance $L$ can be two to three times the burner radius. To determine the appropriate burner size, $R_b$, guidelines have been developed to optimize for the desired thermal input range, turndown, fuel pressure, fan power (pressure drop), combustion chamber size, and other physical constraints. The criterion for minimum thermal input is a bulk flow velocity of $U_0 = 3\,\text{m/s}$. This is simply the flashback point for natural gas ($U_0 \approx 1.7\,\text{m/s}$) with a built-in safety factor. There is no restriction on the maximum thermal input owing to the high turndown (at least 20) available. To optimize for the fuel pressure and fan power, the drag coefficient for different $R$ can be used. The optimum enclosure radius for the LSB is between three and four times $R_b$. Smaller enclosures restrict flow divergence and force the flame to move inside the burner. Larger enclosures allow the flame to over-expand and generate internal flow patterns that affect emissions. We have found these rules and guidelines easy to apply, as they are quite lenient in providing many design options to build simple and low-cost LSBs for integration into existing or new systems.

### 6.3.3.2. Development of a Commercial LSB

Subsequent to the development of LSBs for pool heaters, several projects were pursued to adapt the LSB to industrial and commercial heaters. These studies proved

that the LSB design is robust with regards to application. To investigate turndown, the smallest LSB with $R_b = 2.54$ cm was fired in the open (no enclosure). It generated stable flames from 10 to 600 kW that remained stationary despite the 60:1 change in input rate. At the lowest thermal input of 10 kW, the bulk flow velocity $U_o$ corresponded to 1.7 m/s. This is the minimum allowable operating point for natural gas. Flashback becomes likely if $U_o$ is reduced further because the velocity at the burner exit would be too close to $S_T$. The minimum $U_o$ criterion to prevent flashback also applies to larger burners because the LSB has constant velocity scaling. This simply means that the thermal input of the LSB is directly proportional to $U_o$ and $R_b^2$. The effects of enclosure geometry on LSB performance were also investigated by testing various versions of the $R_b = 6.35$ cm LSB in boilers and furnaces at 150 kW–2.3 MW. The results showed that vane shape and screen placement have little effect on flame noise, flame stability, and lean blow-off. Most significantly, emissions of $NO_x$ depend primarily on $\phi$. As shown in Figure 6.6 by the $NO_x$ emissions from LSBs of various sizes, the trends with $\phi$ are similar despite differences in thermal inputs and combustor geometries. Additional tests of the 6.35 cm LSB were also performed with alternate fuels including natural gas diluted with up to 40% flue gases, and with refinery gases with hydrogen constituent up to 50% to show its capability to accept different fuels. Hydrogen can be a particularly challenging fuel to blend because of its dramatic effect on flame speed (see Chapter 8).

In 2003, Maxon Corporation demonstrated an industrial implementation of LSBs called M-PAKT burners. These products were developed for direct process heat applications of 0.3–1.8 MW (1–6 MM Btu/h) with a guarantee of 4–7 ppm $NO_x$ and CO (both at 3% $O_2$) throughout its 10:1 turndown range. These ultra-low emissions meet the most stringent air-quality rules in the United States. As shown by the schematic in Figure 6.7, the M-PAKT burner has a very simple and compact design consisting of a swirler with air supplied by a blower through a plenum, and a multi-port natural gas injector delivering fuel just upstream of the swirler. The control system is also standard with conventional mechanical linkages and flow dampeners. The performance of these commercial LSBs demonstrated that the implementation of low-swirl combustion can
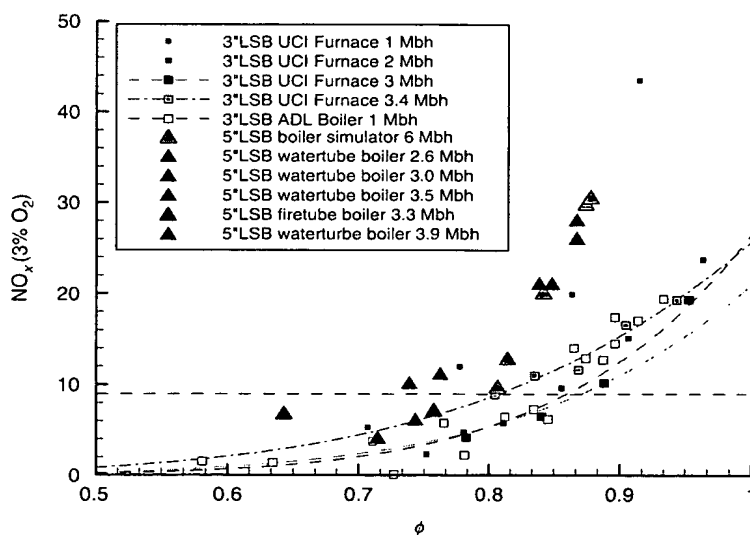


**Figure 6.6**  $NO_x$ emissions of LSB in furnaces and boilers of 300 kW to 1.8 MW. (See color insert.)
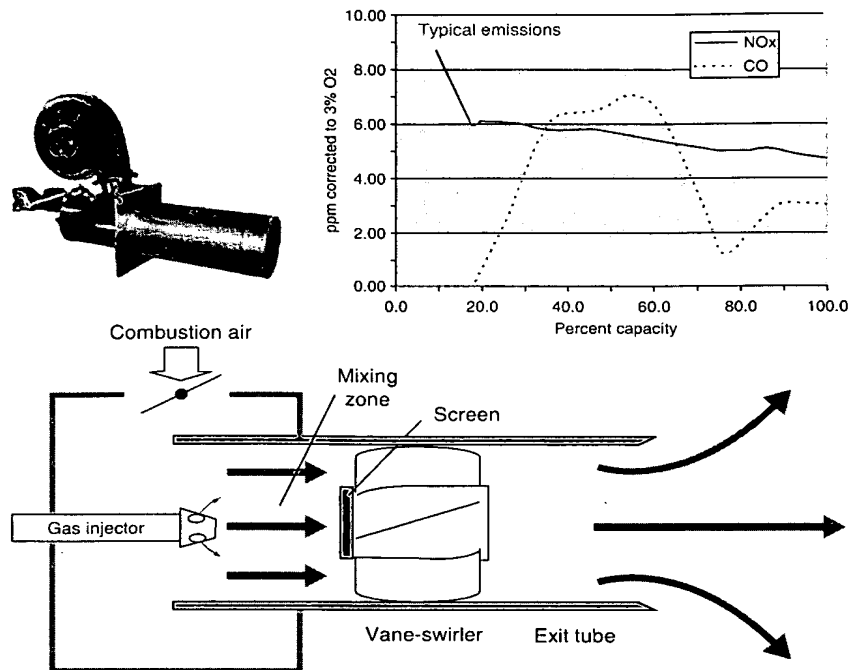
**Figure 6.7** Emissions and schematic of a commercial LSB manufactured by Maxon Corporation of Muncie, Indiana.

not only provide very effective emissions control, but can also improve system performance and reliability by eliminating the need for elaborate controls and intricate auxiliary components. The economic and operational benefit of this approach is significant. Continuing efforts by Maxon to commercialize low-swirl combustion technology include the design of a new LSB product of 15 MW (50 MM Btu/h). The first installation was complete in February of 2005. This large burner has a radius $R_b$ of 25.4 cm and has a 20:1 turndown. It also incorporates a liquid fuel injector for dual-fuel firing. Commercial demonstrations of LSB technology over a range of scales indicate that the fluid mechanics of these burners exhibits some form of self-similarity that is advantageous for burner design. Detailed studies of this similarity can provide insights for future designs.

### 6.3.3.3. Flowfield Characteristics, Turbulent Flame Speed and their Relevance to LSB Performance

The advent of PIV has greatly facilitated the characterization of LSB flowfields by providing the data needed to explain how the LSB delivers consistent performance over a large range of conditions. PIV measures velocity distributions in 2D over a relatively large region and is a much quicker method than LDV for investigating the overall flowfield features. In a recent study, a series of experiments were conducted to compare the flowfield and flame features with increasing $U_0$. Shown in Figure 6.8 is an example of the velocity vectors and turbulence stresses for an LSB with $S = 0.53$, $R_b = 2.54$ cm, $R = 0.6$, $\alpha = 37°$, and $L = 6.3$ cm burning a methane/air flame of $\phi = 0.8$ and $U_0 = 5.0$ m/s. The leading edge of the flame brush is outlined by the
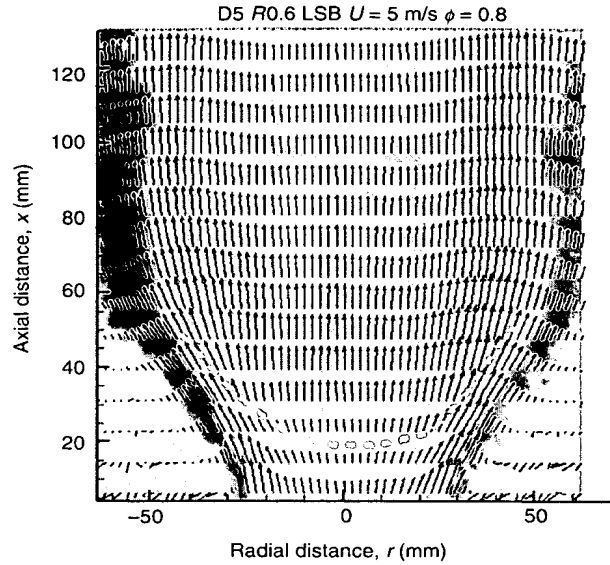
**Figure 6.8** Velocity vectors and turbulence stresses for an LSB burning $CH_4$/air at $\phi = 0.8$ and $U_o = 5.0$ m/s. (See color insert.)

broken line. These velocity vectors show that the LSB flowfield is relatively uniform and free of steep mean velocity gradients. The background contours of the positive (red) and negative (blue) shear stresses also show that high turbulence stresses are confined to the outer edges where the reactants mix with the ambient air. The center flow entering the flame brush is relatively free of large shear stresses. The absence of high stresses means that the flames are much less vulnerable to stress-induced non-uniform heat release and local quenching at ultra-lean conditions. This feature is different than in HSB where steep mean velocity gradients exist in the flame brush and the shear stresses can lead to premature flame blow-off.

As discussed above, $S_T$ is defined in an LSB by the centerline velocity at the leading edge of the flame brush. Figure 6.9 displays values of $S_T$ reported in Cheng *et al.* (2006) for several versions of the LSB with methane, ethylene, propane, and methane diluted with $CO_2$. Despite variations in burner configuration and in ranges of flow conditions, stoichiometry, and fuels, the turbulent flame speed data show an unequivocal linear correlation with $u'$. The only exceptions are three outlying points from the jet-LSB. These results clearly show that the two non-jet implementations of low-swirl combustion, that is, tangential injection swirler and vane swirler, are fully compatible. More importantly, they indicate that the linear behavior of the turbulent flame speed is a characteristic and unique combustion property central to the operation of low-swirl burners.

The evolution of the flowfield with $U_0$ was investigated by applying PIV at $5 < U_0 < 17.5$ m/s. Figure 6.10 presents the normalized axial velocity profiles from the non-reacting cases. The fact that the profiles of the normalized axial velocity, $U/U_0$, and the normalized two-component turbulent kinetic energy, $q'/U_0$ (where $q' = [(u'^2 + v'^2)/2]^{1/2}$), collapse to their respective trends shows that the LSB flowfield exhibits a similarity feature. Similarity is also shown by the radial profiles of $U/U_0$ and $V/U_0$, meaning that the key flowfield features are preserved at different bulk flow
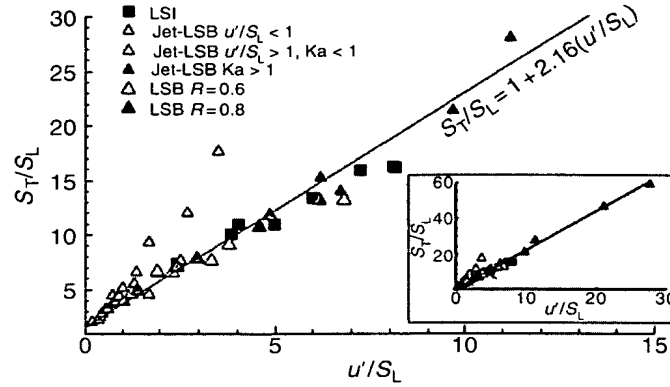
**Figure 6.9** Turbulent flame speed correlation. (See color insert.)
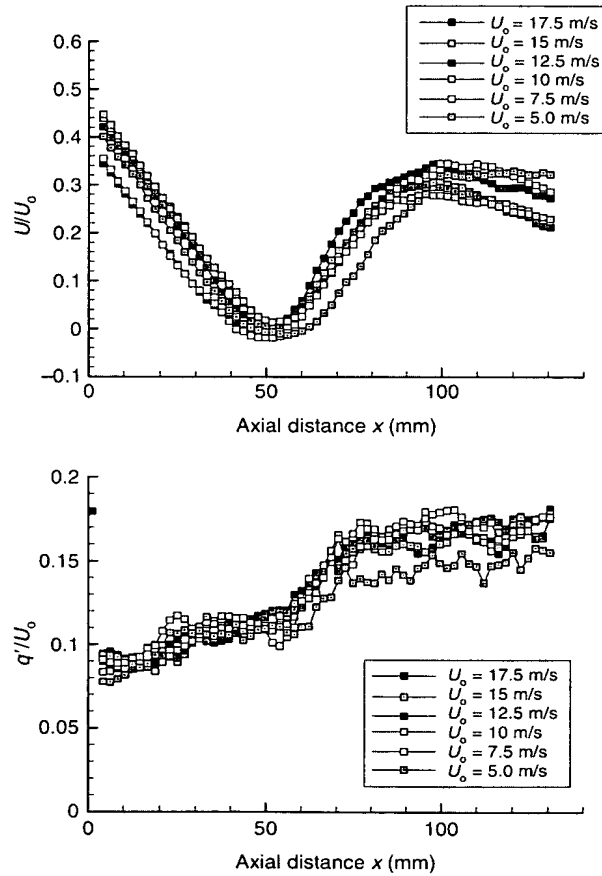


**Figure 6.10** Normalized centerline profiles of non-reacting flow produced by a laboratory LSB showing self-similarity features. (See color insert.)

velocities. Recent PIV measurements in the reacting flowfields of a low-swirl injector developed for gas turbines show that self-similarity is also preserved in the nearfield divergent region (Cheng *et al.*, 2006). The effect of combustion heat release is to increase the aerodynamic stretch rate and decrease $x_0$.

Self-similarity explains why the flame maintains a relatively fixed position regardless of $U_o$. This is illustrated by invoking an equality at the leading edge position of the flame brush, $x_f$, (typically at $15 < x < 25$ mm for this LSB):

$$U_o - \frac{dU}{dx}(x_f - x_o) = S_T. \qquad (6.7)$$

Here, $x_o$ is the virtual origin of the linearly divergent portions of the axial profiles and has a negative value. As discussed earlier, $S_T$ of the LSB is linearly dependent on the rms velocity of the turbulence $u'$ such that $S_T = S_L(1 + Ku')$, where $S_L$ is the laminar flame speed and $K$ is an empirical correlation constant that is 2.16 for methane. Substituting this into Equation (6.4) and dividing both sides by $U_o$ results in

$$1 - \frac{dU}{dx}\frac{(x_f - x_o)}{U_o} = \frac{S_T}{U_o} = \frac{S_L}{U_o} + \frac{Ku'}{U_o}. \qquad (6.8)$$

The similarity feature of the $U/U_o$ profiles means that the normalized axial divergence rate [i.e., $(dU/dx)/U_o$] has a constant value. On the right hand side (RHS), $Ku'/U_o$ is a constant because turbulence produced by the perforated plate is nearly isotropic. The first term of the RHS tends to a very small value for large $U_o$ because the laminar flame speeds for hydrocarbons are from 0.2 to 0.8 m/s. As long as flow similarity is preserved, the flame position at large $U_o$ tends to an asymptotic value independent of the laminar flame speed. This provides an explanation why the lifted flames generated by LSBs do not show significant flame shift during turndown. Flame shift is found only when operating the burner at a $U_o$ that is on the same order as $S_L$. Equation (6.8) also shows that the flame moves closer to the burner exit with decreasing $U_o$ until flashback occurs when $x_f - x_o = 0$.

## 6.4.  SUMMARY

Lean premixed burners can be deceptively simple devices that must nevertheless provide flame stability (i.e., resistance to flashback and blow-off) over the desired range of turndown ratio, and they must maintain this stability with varying fuel composition (even when the fuel is nominally "natural gas"). The reliance on blowers or fans to provide high volume flows of air economically can make these burners' performance very sensitive to fluctuations in fuel composition, particularly when operating fuel lean. High swirl and surface stabilization have two mechanisms to achieve reliable combustion behavior, but turndown can be limited. The relatively new low-swirl approach, on the other hand, has shown great promise in expanding the stability map of lean premixed burners.

## REFERENCES

*AGA Bulletin* #10 (1940). Research in fundamentals of atmospheric gas burner design.
Bedat, B. and Cheng, R.K. (1995). *Combust. Flame* 100, 485–494.
Beer, J.M. and Chigier, N.A. (1972). *Combustion Aerodynamics*. Applied Science Publishers Ltd., London.
Botha, J.P. and Spaulding, D.B. (1954). *Proc. R. Soc. London A* 225, 71–96.
Bouma, P.H. and de Goey, L.P.H. (1999). *Combust. Flame* 119, 133–143.

Bowman, C.T. (1992). *Proc. Combust. Inst.* **24**, 859–878.

Chan, C.K., Lau, K.S., Chin, W.K., and Cheng, R.K. (1992). *Proc. Combust. Inst.* **24**, 511–518.

Cheng, R.K. (1995). *Combust. Flame* **101**, 1–14.

Cheng, R.K. and Yegian, D.T. (1999). Mechanical Swirler for a Low-NO$_x$ Weak-Swirl Burner, US Patent #5879148.

Cheng, R.K., Yegian, D.T., Miyasato, M.M., Samuelsen, G.S., Pellizzari, R., Loftus, P., and Benson, C. (2000). *Proc. Combust. Inst.* **28**, 1305–1313.

Cheng, R.K., Shepherd, I.G., Bedat, B., and Talbot, L. (2002). *Combust. Sci. Technol.* **174**, 29–59.

Cheng, R.K., Littlejohn, D., Nazeer, W.A., and Smith, K.O. (2006). Power for land sea and air, ASME Paper GT2006-90878. *ASME Turbo Expo 2006*, Barcelona, Spain.

Chigier, N.A. and Beer, J.M. (1964). *Trans. ASME, J. Basic Eng.* **4**, 788–796.

Cho, P., Law, C.K., Cheng, R.K., and Shepherd, I.G. (1988). *Proc. Combust. Inst.* **22**, 739.

Davies, T.W. and Beer, J.M. (1971). *Proc. Combust. Inst.* **13**, 631–638.

de Goey, L.P.H., Plessing, T., Hermanns, R.T.E., and Peters, N. (2005). *Proc. Combust. Inst.* **30**, 859–866.

Gupta, A.K., Beer, J.M., and Swithenbank, J. (1978). *Combust. Sci. Technol.* **17**, 199–214.

Harris, J.A. and South, R. (1978). *Gas Eng. Manag.* **May**, 153.

Kortschik, C., Plessing, T., and Peters, N. (2004). *Combust. Flame* **136**, 43–50.

Kostiuk, L.W., Bray, K.N.C., and Cheng, R.K. (1993). *Combust. Flame* **92**, 396–409.

Lilley, D.G. (1977). *AIAA J.* **15**, 1063–1078.

Marcogaz Ad Hoc Working Group on Gas Quality (2002). *National Situations Regarding Gas Quality*, Report UTIL-GQ-02-19, http://marcogaz.org/information/index_info4.htm.

Mokhov, A.V. and Levinsky, H.B. (1996). *Proc. Combust. Inst.* **26**, 2147–2154.

Mokhov, A.V. and Levinsky, H.B. (2000). *Proc. Combust. Inst.* **28**, 2467–2474.

Plessing, T., Kortschik, C., Mansour, M.S., Peters, N., and Cheng, R.K. (2000). *Proc. Combust. Inst.* **28**, 359–366.

Rumminger, M.D., Dibble, R.W., Heberle, N.H., and Crosley, D.R. (1996). *Proc. Combust. Inst.* **26**, 1755–1762.

Shepherd, I.G., Cheng, R.K., Plessing, T., Kortschik, C., and Peters, N. (2002). *Proc. Combust. Inst.* **29**, 1833–1840.

Syred, N. and Beer, J.M. (1974). *Combust. Flame* **23**, 143–201.

von Elbe, G. and Grumer, J. (1948). *Ind. Eng. Chem.* **40**, 1123.

Wobbe, G. (1926). *L'Industria de Gas e degli Acquedotti* **30**, November.

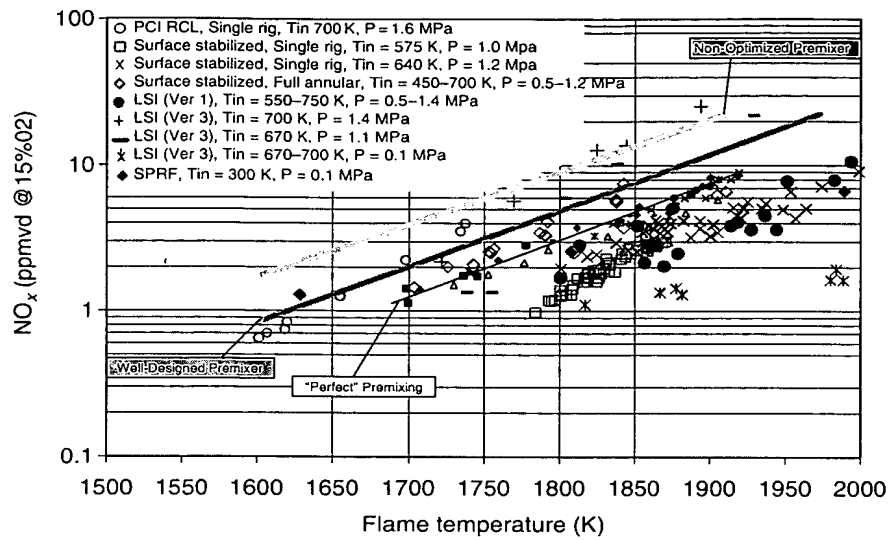Yegian, D.T. and Cheng, R.K. (1998). *Combust. Sci. Technol.* **139**, 207–227.

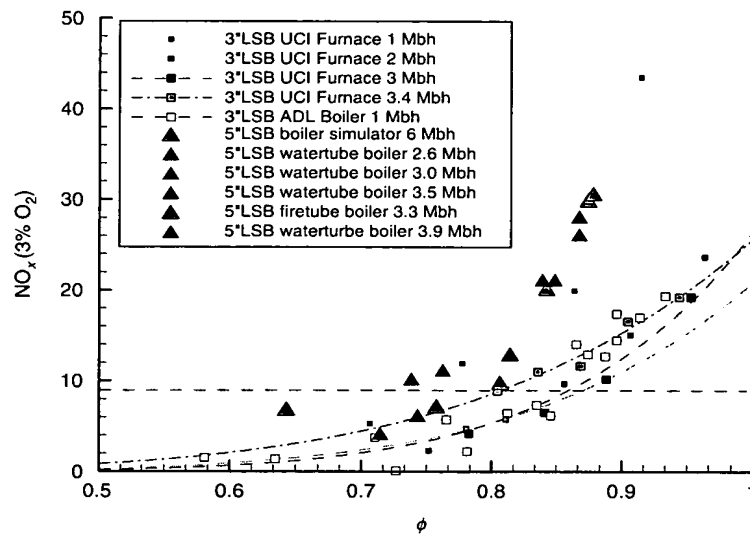**Figure 5.34** NO_x Emissions for various advanced lean premixed strategies for stationary power.



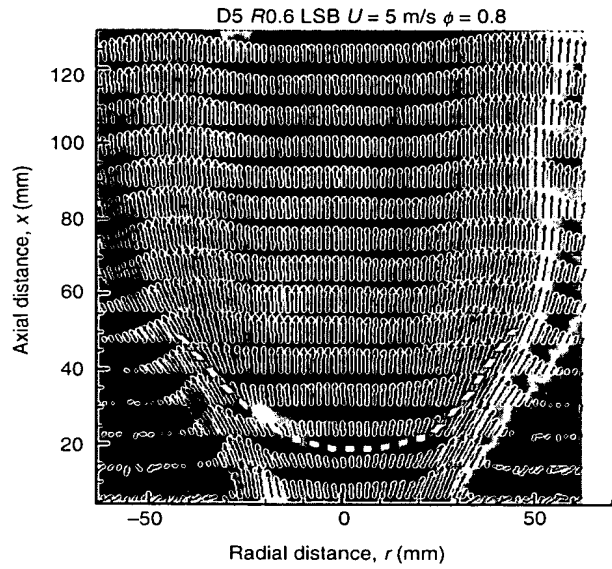**Figure 6.6** NO_x emissions of LSB in furnaces and boilers of 300 kW to 1.8 MW.

**Figure 6.8** Velocity vectors and turbulence stresses for an LSB burning $CH_4$/air at $\phi = 0.8$ and $U_o = 5.0$ m/s.
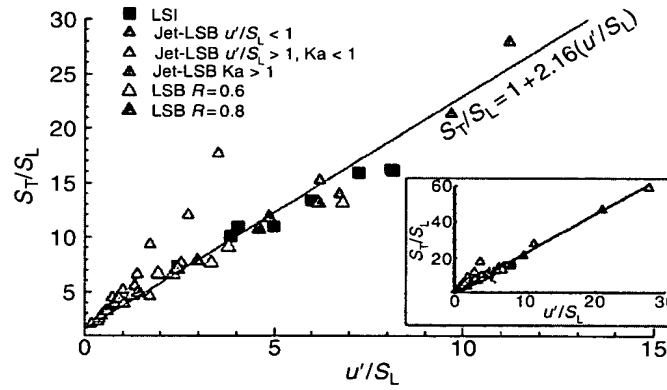


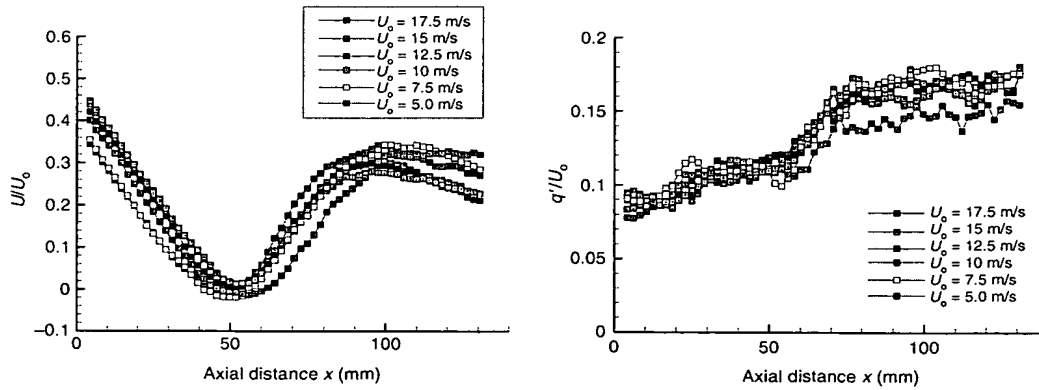**Figure 6.9** Turbulent flame speed correlation.



**Figure 6.10** Normalized centerline profiles of non-reacting flow produced by a laboratory LSB showing self-similarity features.